Adsorption characteristics of Cu^{2+} on $NiFe_2O_4$ magnetic nanoparticles

Farid Moeinpour and Shohreh Kamyab

ABSTRACT

Magnetic $NiFe_2O_4$ nanoparticles have been synthesized and used as adsorbents for copper removal from aqueous solution. The $NiFe_2O_4$ nanoparticles were characterized by scanning electron microscope, transmission electron microscope, X-ray diffraction, and Fourier transform infrared spectroscopy. The batch removal of Cu^{2+} ions from aqueous solutions using $NiFe_2O_4$ magnetic nanoparticles under different experimental conditions was investigated. The effects of initial concentration, adsorbent dose, contact time, and pH were investigated. The adsorption process was pH dependent, and the maximum adsorption was observed at a pH of 6.0. Equilibrium was achieved for copper ion after 25 min. Experimental results showed that $NiFe_2O_4$ magnetic nanoparticles are effective for the removal of copper ions from aqueous solutions. The pseudo-second-order kinetic model gave a better fit of the experimental data as compared to the pseudo-first-order kinetic model. Experimental data showed a good fit with the Langmuir isotherm model.

Key words | adsorption, copper contamination, magnetic separation, $NiFe_2O_4$ nanoparticles

Farid Moeinpour (corresponding author)
Shohreh Kamyab
Department of Chemistry,
Bandar Abbas Branch,
Islamic Azad University,
Bandar Abbas,
Iran
E-mail: *f.moeinpour@gmail.com*

INTRODUCTION

Today, because of industrial development and due to industrial wastewater entering into the environment, ecosystems around factories and also surface and ground waters are in danger of pollution (Nies 1999). The presence of metal ions in wastewater and surface water is one of the main concerns to human health and the environment. The excessive use of metals and chemical materials in industrial processes causes wastewater with high percentages of metal ions (Nasiruddin Khan & Farooq Wahab 2007). Copper is an essential element for plants and animals, but an excess is toxic. Human activities, such as mining, melting, usage of industrial and domestic sludge sewage on agricultural land, and also the use of copper in fungicides and insecticides, cause contamination of water and soil (Xu *et al.* 2006). Excessive concentration of copper in the human body can lead to gastrointestinal diseases (Nasiruddin Khan & Farooq Wahab 2007). The maximum acceptable concentration of copper in drinking water is 1.5 ppm as recommended by the World Health Organization (Karabulut *et al.* 2000). Common methods for removing metals from wastewater include chemical precipitation, ion exchange, adsorption by activated carbon, and electrolytic processes (Leyva-Ramos *et al.* 2005). Among several chemical and physical methods, the adsorption process is an effective technique that has been successfully employed for heavy metal removal from wastewater (Mohammed *et al.* 2011). Various adsorbents have been reported for the removal of Cu(II) from aqueous solutions, including zeolite (Zhang *et al.* 2011), diatomite (Safa *et al.* 2012), kaolinite (Guerra *et al.* 2008), chitosan (Juang *et al.* 1999), alumina (Rajurkar *et al.* 2011), functionalized polymers (Zhou *et al.* 2009), and zero-valent iron (Karabelli *et al.* 2008). However, most of these adsorbents are not the ideal choices due to their low adsorption capacity, inadequate adsorption efficiencies, complication separations from the solutions, or high costs.

In recent years, magnetic nanoparticles have attracted much attention because of their widespread application in different fields, such as mineral separation magnetic storage devices, catalysis, magnetic refrigeration systems,

doi: 10.2166/wrd.2014.020

heat transfer application in drug delivery system, magnetic resonance imaging, cancer therapy, and magnetic cell separation (Liu *et al.* 2004; Sharma & Srivastava 2009; Hasany *et al.* 2013; Lee *et al.* 2013; Mody *et al.* 2014; Sobhani *et al.* 2014). The application of magnetic nanoparticles in wastewater treatment is becoming an interesting area of research (Hu *et al.* 2006; Banerjee & Chen 2007; Liu *et al.* 2008; Wang *et al.* 2009; White *et al.* 2009). Nanoparticles exhibit good adsorption efficiency, especially due to the higher surface area and more active sites for interaction with metallic species and dyes, and they can easily be synthesized (Mak & Chen 2005). Among the various magnetic nanoparticles, Ni ferrites with the general formula (AB_2O_4) are one of the most versatile materials as they have high saturation magnetization, high Curie temperature, and chemical stability (Goldman 2006). $NiFe_2O_4$ magnetic nanoparticles as a low cost, nontoxic adsorbent, containing active functional hydroxyl groups, are selected for their better application to and management of wastewater remediation. The objectives of this study are: (1) the synthesis of $NiFe_2O_4$ magnetic nanoparticles by the co-precipitation method (Zins *et al.* 1999) and their characterization with respect to scanning electron microscopy (SEM), transmission electron microscopy (TEM), X-ray diffraction (XRD), and Fourier transform infrared spectroscopy (FT-IR); (2) a comparative batch adsorption study of the adsorbent for Cu^{2+} with respect to various environmental parameters (initial concentration, adsorbent dose, contact time, and pH); and (3) corresponding isotherm and kinetic studies.

MATERIALS AND METHODS

Analytical-grade $Cu(NO_3)_2.5H_2O$ was obtained from Merck. A 1,000 mg/L stock solution of the salt was prepared in deionized water. All working solutions were prepared by diluting the stock solution with deionized water. Deionized water was prepared using a Millipore Milli-Q (Bedford, MA, USA) water purification system. All reagents ($FeCl_3$, $NiCl_2$, ammonium hydroxide (29.6%), NaOH, NaCl, and HNO_3) used in the study were of analytical grade and purchased from Aldrich. Before each experiment, all glassware was cleaned with dilute nitric acid and repeatedly washed with deionized water.

XRD analysis was carried out using a PAN analytical X'Pert Pro X-ray diffractometer. Surface morphology and particle size were studied using a Hitachi S-4800 SEM instrument. TEM was performed using a Hitachi H-7650 microscope at 80 kV. FT-IR spectra were determined as KBr pellets on a Bruker model 470 spectrophotometer. All the metal ion concentrations were measured with a Varian AA240FS atomic absorption spectrophotometer.

Preparation of the $NiFe_2O_4$

The solution of metallic salts $FeCl_3$ (160 mL, 1 M) and $NiCl_2$ (40 mL, 1 M) was poured as quickly as possible into a boiling alkaline solution [NaOH (1,000 mL, 1 M)] under vigorous stirring. Then, the solution was cooled and continuously stirred for 90 min. The resulting precipitate was then purified by a four-times-repeated centrifugation (4,000–6,000 rpm, 20 min) and decantation (Zins *et al.* 1999).

Adsorption experiments

Batch adsorption of copper ions onto the adsorbent ($NiFe_2O_4$) was investigated in aqueous solutions under various operating conditions: pH 2–6, at a temperature of 298 K, for an initial Cu^{2+} ion concentration of 4 mg/L. About 0.05 g adsorbent was added to 20 mL of copper nitrate solution (4 mg/L). Then, the mixture was agitated on a shaker at 250 rpm. The initial pH values of the copper solutions were adjusted from 2 to 6 with 0.1 mol L^{-1} HNO_3 or 0.1 mol L^{-1} NaOH solutions using a pH meter. After equilibrium, the samples were centrifuged and the adsorbent ($NiFe_2O_4$) removed magnetically from the solution. The Cu(II) concentration in the supernatant was measured by flame atomic absorption spectrometer. The effects of several parameters, such as contact time, initial concentration, pH, and adsorbent dose, on the extent of adsorption of Cu(II) were investigated.

The Cu(II) removal percentage was calculated as Equation (1):

$$\% \text{ removal} = \frac{C_0 - C_t}{C_0} \times 100 \quad (1)$$

where C_0 and C_t (mg/L) are the concentration of Cu(II) in the solution at initial and equilibrium time, respectively.

The amount of Cu(II) adsorbed (Q_e) was calculated using Equation (2):

$$Q_e = \frac{(C_0 - C_t)V}{m} \quad (2)$$

where C_0 and C_t are the initial and equilibrium concentrations of Cu(II) (mg/L), m is the mass of $NiFe_2O_4$ nanoparticles (g), and V is the volume of solution (L).

Adsorption isotherms

Adsorption isotherms were obtained by using 0.05 g of adsorbent and 20 mL of copper nitrate solution with different concentrations (4–60 mg/L) at 298 K. These solutions were buffered at an optimum pH (pH = 6) for adsorption and agitated on a shaker at 250 rpm until they reached adsorption equilibrium (25 min). The quantity of Cu(II) adsorbed was derived from the concentration change.

RESULTS AND DISCUSSION

Characterization of $NiFe_2O_4$ magnetic nanoparticles

$NiFe_2O_4$ nanocrystallites were prepared according to the reported procedure (Zins *et al.* 1999). $NiFe_2O_4$ nanocrystallites were characterized by FT-IR (Figure 1), XRD (Figure 2), TEM (Figure 3), and SEM (Figure 4). The FT-IR spectrum of $NiFe_2O_4$ (Figure 1) exhibits strong bands in the low-frequency region (1,000–500 cm^{-1}) due to the iron oxide skeleton, which is consistent with the magnetite spectrum (Pol *et al.* 2009). The peak at 1,633 cm^{-1} showed the existence of Fe–O, and the peak at 3,446 cm^{-1} implied the existence of residual hydroxyl groups (Pol *et al.* 2009). To confirm the Ni ferrite formation in the synthesized magnetic nanoparticles, the XRD pattern of the sample was studied. The XRD pattern in Figure 2 shows that these nanoparticles have spinel structure, with all major peaks matching the standard pattern of bulk $NiFe_2O_4$ (JCPDS 10-325). The TEM and SEM photographs of the sample are illustrated in Figures 3 and 4, respectively. Both the SEM and TEM

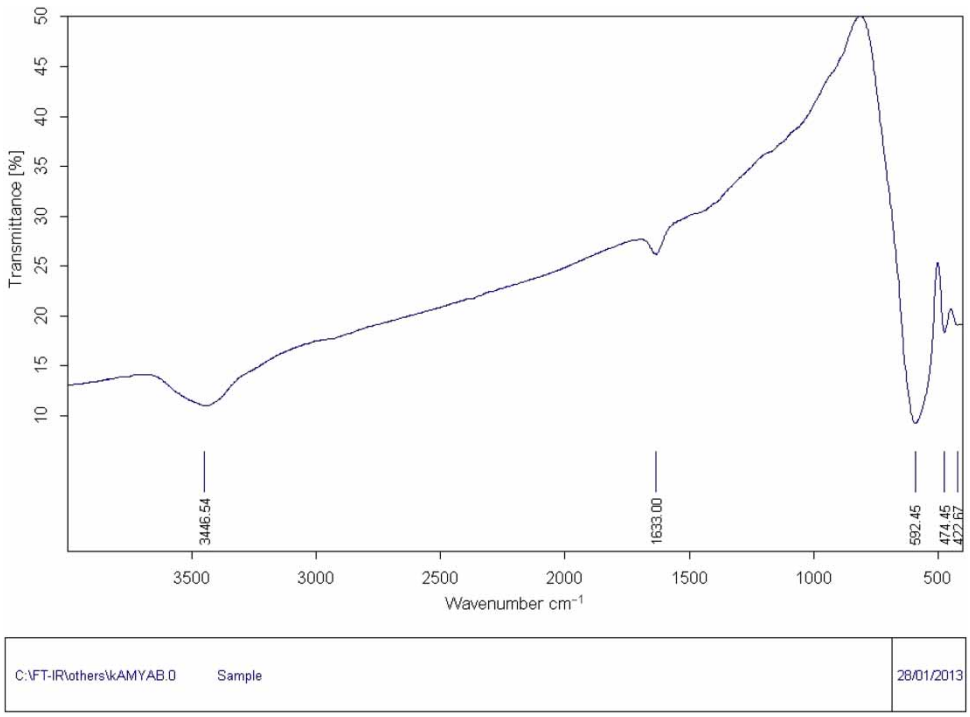

Figure 1 | The FT-IR spectrum of $NiFe_2O_4$ nanoparticles.

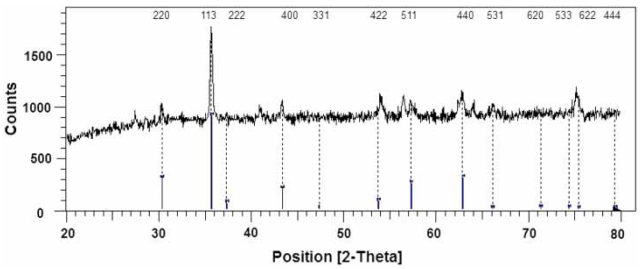

Figure 2 | XRD pattern of $NiFe_2O_4$ nanoparticles.

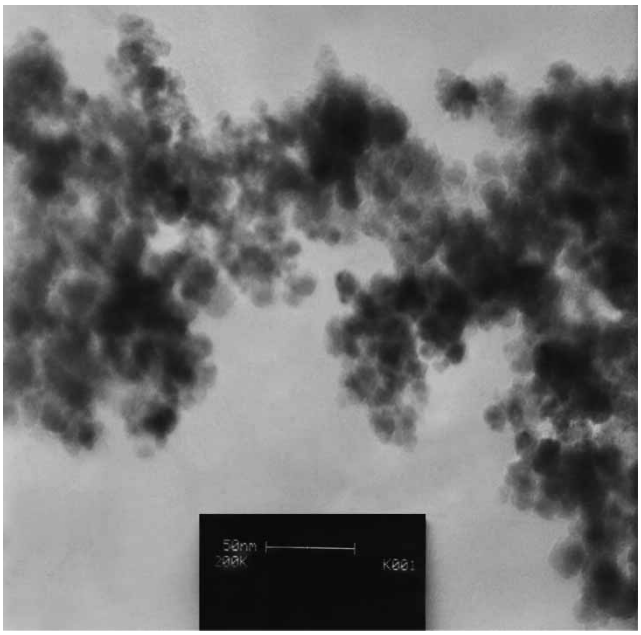

Figure 3 | TEM image of $NiFe_2O_4$ nanoparticles.

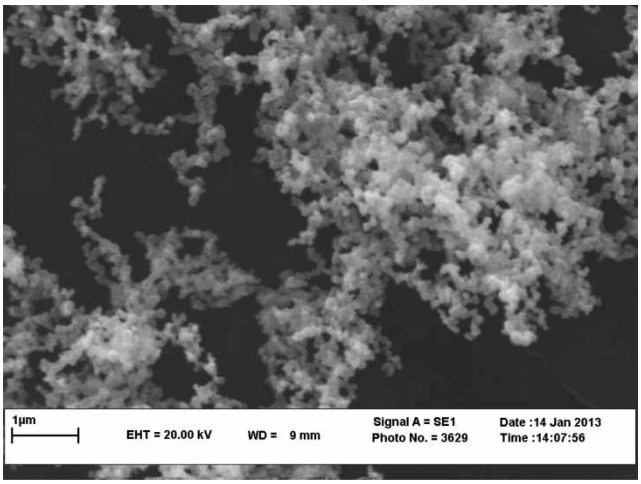

Figure 4 | SEM image of $NiFe_2O_4$ nanoparticles.

images demonstrate that the prepared magnetic nanoparticles are spherical, with average size of <50 nm in the diameter.

Adsorption and removal of copper from aqueous solution

Effect of pH

The acidity of the aqueous solution exerts a significant influence on the adsorption process, because it can affect the solution chemistry of contaminants and the state of functional groups on the surface of adsorbents (Sheng *et al.* 2010). The effect of solution pH on Cu(II) adsorption was investigated at pH 2–6 at 298 K. As shown in Figure 5, only a small amount of Cu(II) is adsorbed onto the adsorbent at pH = 2. The adsorption amount of Cu(II) increases with increasing pH values from 2 to 6. Cu(II) in aqueous solution can be present in several forms, such as $Cu(H_2O)_6^{+2}$, $Cu(OH)^{+}$, $Cu(OH)_2$, $Cu(OH)_3^{-}$, and $Cu(H_2O)_6^{+2}$; $Cu(H_2O)_6^{+2}$ is the predominant species at pH < 6.0 (Sheng *et al.* 2010). The adsorption experiments at pH > 6 were not studied because of the precipitation of $Cu(OH)_2$ in the solution. Thus, the optimum pH for Cu(II) ion sorption is found in the pH range of 5–6, which is in accordance with previous reports (Wang *et al.* 2011; Xin *et al.* 2012). The subsequent experiments were carried out at pH 6.0.

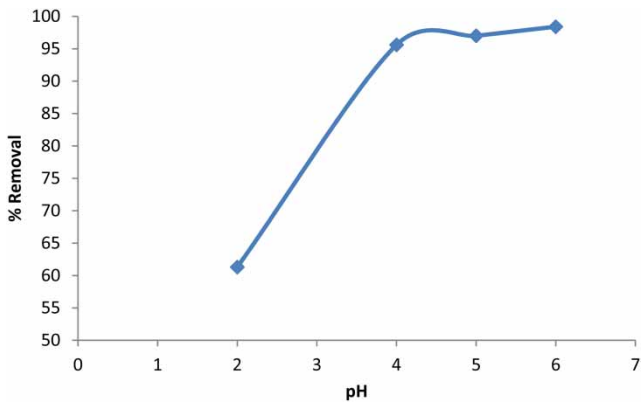

Figure 5 | Percentage of copper removal at different pH values (initial Cu(II) concentration = 4 mg/L, adsorbent dose = 0.05 g, and T = 298 K).

Effect of contact time

The effect of contact time on the amount of copper adsorbed was investigated at 4 mg/L initial concentration of copper. It could be observed from Figure 6 that with the increase of contact time, the percentage adsorptions also increased. Minimum adsorption was 91.75% for the time 5 min to maximum adsorption value 98.30% for the time 25 min. The adsorption characteristic showed a rapid uptake of the copper. The adsorption rate, however, decreased to a constant value with an increase in contact time, because all available sites were covered, and no active site was present for binding.

Effect of the adsorbent dosage

The effect of the adsorbent amount on the copper adsorption was studied, with the adsorbent amount ranging from 0.01 to 0.2 g. The results obtained are shown in Figure 7. From Figure 7, it is observed that the most suitable adsorbent dosage is 0.05 g. As the adsorbent dose increases, the percentage removal also increases, until it reaches a saturation point, where the increase in adsorbent does not change the percentage removal significantly.

Effect of initial Cu(II) concentration

The effects of initial Cu(II) concentrations at the range values from 4 to 60 mg/L on the adsorption of copper were investigated. As shown in Figure 8, the percentage of removal decreased with the increase in Cu(II) concentration. At higher Cu(II) concentrations, the ratio of available adsorbent surface to the initial Cu(II) concentration is low and the percentage of removal then depends upon the initial concentration.

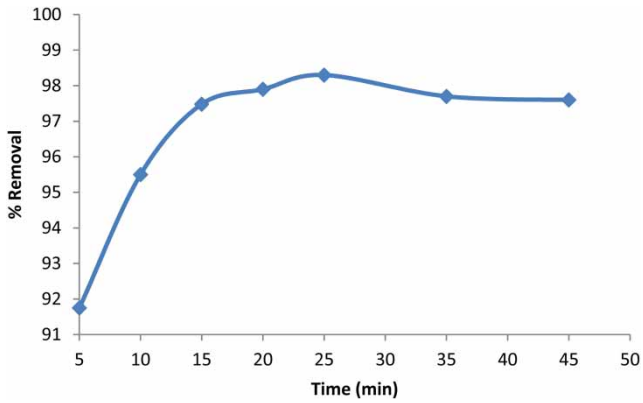

Figure 6 | Effect of contact time (initial Cu(II) concentration = 4 mg/L, adsorbent dose = 0.05 g, pH = 6, and T = 298 K).

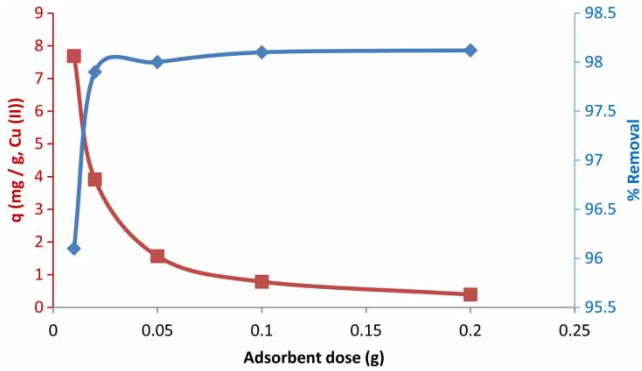

Figure 7 | The effect of adsorbent dosage on the removal percentage of Cu(II) ions (initial Cu(II) concentration = 4 mg/L, pH = 6, contact time = 25 min, and T = 298 K).

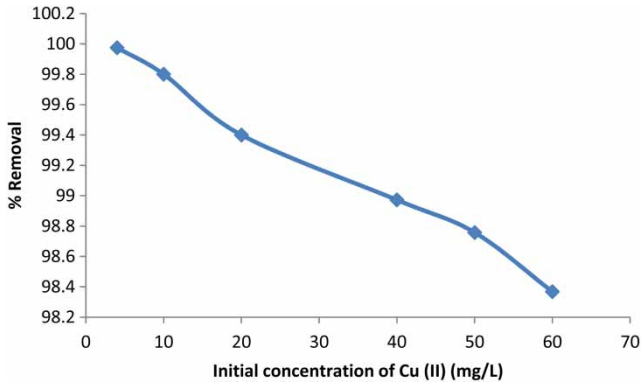

Figure 8 | Effect of initial Cu(II) concentration on the removal of Cu(II) (adsorbent dose = 0.05 g, pH = 6, contact time = 25 min, and T = 298 K).

Adsorption isotherms

The experimental data were correlated by Langmuir and Freundlich models. The related linear equations are shown in Equations (5) and (6), respectively.

Langmuir equation:

$$\frac{C_e}{q_e} = \frac{1}{k_a q_m} + \frac{C_e}{q_m} \tag{3}$$

where q_e is the amount of Cu^{2+} adsorbed per unit mass at equilibrium (mg/g); q_m is the maximum amount of

adsorbent that can be adsorbed per unit mass adsorbent (mg/g); C_e is concentration of adsorbent (in the solution at equilibrium (mg/L)); and k_a is adsorption equilibrium constant.

A plot of C_e/q_e versus C_e gives a straight line, with a slope of $1/q_m$ and intercept $1/k_a q_m$.

Freundlich equation:

$$\log q_e = \log K_F + \frac{1}{n}\log C_e \quad (4)$$

where C_e (mg/L) and q_e (mg/g) are the equilibrium concentration of adsorbent in the solution and the amount of adsorbent adsorbed at equilibrium, respectively; K_F ($mg^{1-(1/n)}$ $L^{1/n}$ g^{-1}) and n are the Freundlich constants, which show the adsorption capacity for the adsorbent and adsorption intensity, respectively.

A plot of $\log q_e$ versus $\log C_e$ gives a straight line of slope $1/n$ and intercept $\log K_F$.

If $(1/n) < 1$, then the adsorption is favorable. If $(1/n) > 1$, the adsorption bond becomes weak and unfavorable adsorption occurs.

At first, we correlated the adsorption data at different initial concentrations of Cu(II) ion in terms of the Langmuir isotherm (Equation (3)). Furthermore, we examined the data according to the Freundlich isotherm (Equation (4)). The calculated parameters of the Langmuir and Freundlich models are given in Table 1 and Figure 9. The comparison of correlation coefficients (R^2) of the linearized form of both equations indicates that the Langmuir model yields a better fit for the experimental equilibrium adsorption data than the Freundlich model. This suggests the monolayer coverage of the surface of $NiFe_2O_4$ nanoparticles by copper ions.

The maximum adsorption capacity is compared in Table 2 with the data reported by other authors for copper adsorption. As can be seen, the maximum copper adsorption value of $NiFe_2O_4$ is higher than those reported in the literature. This comparison shows the great potential of $NiFe_2O_4$ magnetic nanoparticles for the removal of copper from wastewater.

Adsorption kinetics

In this study, pseudo-first-order and pseudo-second-order kinetics models were applied to examine the controlling mechanism of copper ions' adsorption from aqueous solutions. Adsorption equilibrium was reached in 25 min (Figure 6). The linear form of the pseudo-first-order model and pseudo-second-order kinetics model can be described as shown in Equations (5) and (6), respectively:

$$\ln(q_e - q_t) = \ln q_e - k_1 \cdot t \quad (5)$$

$$\frac{t}{q_t} = \frac{1}{k_2 q_e^2} + \frac{t}{q_e} \quad (6)$$

where q_e and q_t are the adsorption capacities at equilibrium and at time t (min), respectively. k_1 (min^{-1}) and k_2 (g/(mg.min)) are the pseudo-first-order and pseudo-second-order rate constants, respectively (Ho 2006). The equilibrium experimental results were not well fitted with the pseudo-first-order model (Table 1). The values of q_e and k_2 can be calculated from the

Table 1 | Isotherm and kinetic model parameters for the Cu(II) adsorption on $NiFe_2O_4$ magnetic nanoparticles

Isotherm models

Langmuir			**Freundlich**		
R^2	q_m (mg/g)	k_a (L/mg)	R^2	K_F ($mg^{1-(1/n)}$ $L^{1/n}$ g^{-1})	$1/n$
0.9985	200	2.5	0.9032	9.22	0.8684

Kinetic models

Pseudo first-order			**Pseudo second-order**			
R^2	$q_{e,cal.}$ (mg/g)	k_1 (min^{-1})	R^2	$q_{e,exp.}$ (mg/g)	$q_{e,cal.}$ (mg/g)	k_2 (g/(mg.min))
0.646	1.590	0.089	0.999	9.829	9.823	0.531

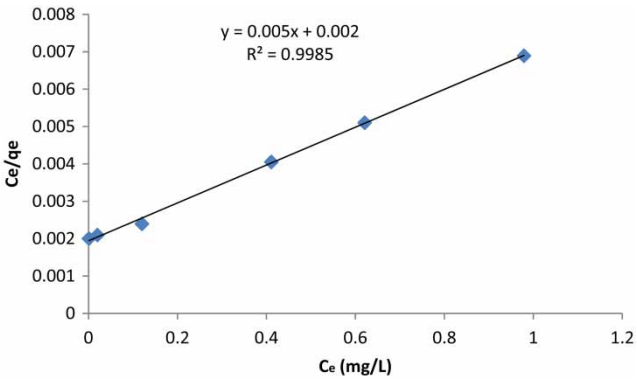

Figure 9 | The Langmuir adsorption isotherm of $NiFe_2O_4$ magnetic nanoparticles (0.05 g) for Cu(II) ions.

Table 2 | Maximum adsorption capacities of copper from aqueous media using various adsorbents

Adsorbents	q_m (mg/g)	References
$NiFe_2O_4$ nanoparticles	200	This study
Hydroxyapatite nanoparticles	36.90	Wang *et al.* (2009)
Maghemite nanoparticle	27.70	Hu *et al.* (2006)
Magnetic gamma-Fe_2O_3 nanoparticles coated with poly-L-cysteine	42.90	White *et al.* (2009)
Fe_3O_4 magnetic nanoparticles coated with humic acid	46.30	Liu *et al.* (2008)
Magnetic nano-adsorbent modified by gum arabic	38.50	Banerjee & Chen (2007)

slope and intercept of the plot of t/q_t versus t (figure not shown). The results listed in Table 1 show that the correlation coefficient is very high ($R^2 = 0.999$). Furthermore, the calculated equilibrium adsorption capacity was consistent with the experimental result. This result suggested that the kinetics data were better described with a pseudo-second-order kinetics model, which supported the assumption that the rate-limiting step may be chemical sorption (Wu *et al.* 2001).

CONCLUSIONS

$NiFe_2O_4$ magnetic nanoparticles with average size less than 50 nm in diameter have been synthesized for efficient removal of copper from water. The prepared magnetic nanoparticles can be easily separated from the solution using an external magnet after adsorption. The following results were obtained in this study: (1) the equilibrium time for the adsorption of the copper ions onto adsorbent was 25 min (initial Cu(II) concentration = 4 mg/L, adsorbent dose = 0.05 g, pH = 6, and $T = 298$ K), and adsorption kinetic data were well described by a pseudo-second-order model with a high correlation coefficient ($R^2 = 0.999$); (2) adsorption isotherm data of $NiFe_2O_4$ were fitted well with the Langmuir model ($q_m = 200$ mg/g, $k_a = 2.5$ L/mg, and $R^2 = 0.9985$); and (3) removal of Cu(II) increases with increasing pH, and a maximum value was found at pH 6.0. At this pH (initial Cu(II) concentration = 4 mg/L, adsorbent dose = 0.05 g, and $T = 298$ K), the removal rate of copper ions was found to be 98.4%. Thus, the process of purifying water pollution presented here is efficient using magnetic nanoparticles.

ACKNOWLEDGEMENT

The authors are grateful to Islamic Azad University, Bandar Abbas Branch for financial support.

REFERENCES

Banerjee, S. S. & Chen, D. H. 2007 Magnetic nanoparticles grafted with cyclodextrin for hydrophobic drug delivery. *Chem. Mater.* **19**, 6345–6349.

Goldman, A. 2006 *Modern Ferrite Technology*. Springer, New York.

Guerra, D. L., Airoldi, C. & de Sousa, K. S. 2008 Adsorption and thermodynamic studies of Cu(II) and Zn(II) on organofunctionalized-kaolinite. *Appl. Surf. Sci.* **254**, 5157–5163.

Hasany, F. S., Abdurahman, H. N., Sunarti, R. A. & Jose, R. 2013 Magnetic iron oxide nanoparticles: chemical synthesis and applications review. *Curr. Nanosci.* **9**, 561–575.

Ho, Y. S. 2006 Review of second-order models for adsorption systems. *J. Hazard. Mater.* **136**, 681–689.

Hu, J., Chen, G. & Lo, I. M. 2006 Selective removal of heavy metals from industrial wastewater using maghemite nanoparticle: performance and mechanisms. *J. Environ. Eng.* **132**, 709–715.

Juang, R. S., Wu, F. C. & Tseng, R. L. 1999 Adsorption removal of copper(II) using chitosan from simulated rinse solutions containing chelating agents. *Water Res.* **33**, 2403–2409.

Karabelli, D., Üzüm, C. A. R., Shahwan, T., Eroğlu, A. E., Scott, T. B., Hallam, K. R. & Lieberwirth, I. 2008 Batch removal of

aqueous Cu^{2+} ions using nanoparticles of zero-valent iron: a study of the capacity and mechanism of uptake. *Ind. Eng. Chem. Res.* **47**, 4758–4764.

Karabulut, S., Karabakan, A., Denizli, A. & Yürüm, Y. 2000 Batch removal of copper(II) and zinc(II) from aqueous solutions with low-rank Turkish coals. *Sep. Purif. Technol.* **18**, 177–184.

Lee, J., Ji-wook, K. & Jinwoo, C. 2013 Magnetic nanoparticles for multi-imaging and drug delivery. *Mol. Cells* **35**, 274–284.

Leyva-Ramos, R., Bernal-Jacome, L. & Acosta-Rodriguez, I. 2005 Adsorption of cadmium(II) from aqueous solution on natural and oxidized corncob. *Sep. Purif. Technol.* **45**, 41–49.

Liu, J. F., Zhao, Z. S. & Jiang, G. B. 2008 Coating Fe_3O_4 magnetic nanoparticles with humic acid for high efficient removal of heavy metals in water. *Environ. Sci. Technol.* **42**, 6949–6954.

Liu, Z., Wang, H., Lu, Q., Du, G., Peng, L., Du, Y., Zhang, S. & Yao, K. 2004 Synthesis and characterization of ultrafine well-dispersed magnetic nanoparticles. *J. Magn. Magn. Mater.* **283**, 258–262.

Mak, S. Y. & Chen, D. H. 2005 Binding and sulfonation of poly (acrylic acid) on iron oxide nanoparticles: a novel, magnetic, strong acid cation nano-adsorbent. *Macromol. Rapid Commun.* **26**, 1567–1571.

Mody, V. V., Cox, A., Shah, S., Singh, A., Bevins, W. & Parihar, H. 2014 Magnetic nanoparticle drug delivery systems for targeting tumor. *Appl. Nanosci.* **4**, 385–392.

Mohammed, F., Roberts, E., Hill, A., Campen, A. & Brown, N. 2011 Continuous water treatment by adsorption and electrochemical regeneration. *Water Res.* **45**, 3065–3074.

Nasiruddin Khan, M. & Farooq Wahab, M. 2007 Characterization of chemically modified corncobs and its application in the removal of metal ions from aqueous solution. *J. Hazard. Mater.* **141**, 237–244.

Nies, D. H. 1999 Microbial heavy-metal resistance. *Appl. Microbiol. Biotechnol.* **51**, 730–750.

Pol, V. G., Daemen, L. L., Vogel, S. & Chertkov, G. 2009 Solvent-free fabrication of ferromagnetic Fe_3O_4 octahedra. *Ind. Eng. Chem. Res.* **49**, 920–924.

Rajurkar, N. S., Gokarn, A. N. & Dimya, K. 2011 Adsorption of chromium(III), nickel(II), and copper(II) from aqueous solution by activated alumina. *Clean Soil Air Water* **39**, 767–773.

Safa, M., Larouci, M., Meddah, B. & Valemens, P. 2012 The sorption of lead, cadmium, copper and zinc ions from aqueous solutions on a raw diatomite from Algeria. *Water Sci. Technol.* **65** (10), 1729–1737.

Sharma, Y. & Srivastava, V. 2009 Separation of Ni(II) ions from aqueous solutions by magnetic nanoparticles. *J. Chem. Eng. Data* **55**, 1441–1442.

Sheng, G., Li, J., Shao, D., Hu, J., Chen, C., Chen, Y. & Wang, X. 2010 Adsorption of copper(II) on multiwalled carbon nanotubes in the absence and presence of humic or fulvic acids. *J. Hazard. Mater.* **178**, 333–340.

Sobhani, S., Mesbah Falatooni, Z. & Honarmand, M. 2014 Synthesis of phosphoric acid supported on magnetic core–shell nanoparticles: a novel recyclable heterogeneous catalyst for Kabachnik–Fields reaction in water. *RSC Adv.* **4**, 15797–15806.

Wang, Y. J., Chen, J. H., Cui, Y. X., Wang, S. Q. & Zhou, D. M. 2009 Effects of low-molecular-weight organic acids on Cu(II) adsorption onto hydroxyapatite nanoparticles. *J. Hazard. Mater.* **162**, 1135–1140.

Wang, X. S., Zhu, L. & Lu, H. J. 2011 Surface chemical properties and adsorption of Cu(II) on nanoscale magnetite in aqueous solutions. *Desalination* **276**, 154–160.

White, B. R., Stackhouse, B. T. & Holcombe, J. A. 2009 Magnetic γ-Fe_2O_3 nanoparticles coated with poly-l-cysteine for chelation of As(III), Cu(II), Cd(II), Ni(II), Pb(II) and Zn(II). *J. Hazard. Mater.* **161**, 848–853.

Wu, F. C., Tseng, R. L. & Juang, R. S. 2001 Enhanced abilities of highly swollen chitosan beads for color removal and tyrosinase immobilization. *J. Hazard. Mater.* **81**, 167–177.

Xin, X., Wei, Q., Yang, J., Yan, L., Feng, R., Chen, G., Du, B. & Li, H. 2012 Highly efficient removal of heavy metal ions by amine-functionalized mesoporous Fe_3O_4 nanoparticles. *Chem. Eng. J.* **184**, 132–140.

Xu, J., Yang, L., Wang, Z., Dong, G., Huang, J. & Wang, Y. 2006 Toxicity of copper on rice growth and accumulation of copper in rice grain in copper contaminated soil. *Chemosphere* **62**, 602–607.

Zhang, L., Zhang, H. & Yu, X. 2011 Investigation of solution chemistry effects on sorption behavior of Cu(II) on ZSM-5 zeolite. *Water Environ. Res.* **83**, 2170–2177.

Zhou, L. C., Li, Y. F., Bai, X. & Zhao, G. H. 2009 Use of microorganisms immobilized on composite polyurethane foam to remove Cu(II) from aqueous solution. *J. Hazard. Mater.* **167**, 1106–1113.

Zins, D., Cabuil, V. & Massart, R. 1999 New aqueous magnetic fluids. *J. Mol. Liq.* **83**, 217–232.

First received 25 March 2014; accepted in revised form 14 July 2014. Available online 27 October 2014